

Prediction of the characteristics of the liquid film in open inclined micro-channels.

Antonios D. ANASTASIOU¹, Noor AL-RIFAI², Asterios GAVRIILIDIS², Aikaterini A. MOUZA^{1*}

* Corresponding author: Tel.:+30 2310 994161; Email: mouza@cheng.auth.gr

¹ Department of Chemical Engineering, Aristotle University of Thessaloniki, Greece

² Department of Chemical Engineering, UCL, UK

Abstract: *Falling Film Microreactor (FFMR)* is one of the most important microfluidic devices for gas-liquid applications. In these devices extended specific surfaces (up to $20,000\text{m}^2/\text{m}^3$) can be obtained while the liquid film remains stable over a wide range of gas and liquid flow rates. In an effort to propose new design correlations for these devices, in a previous work we proposed correlations for the prediction of the gas-liquid interface and the thickness of the liquid film. In this study we aim to investigate the validity of these correlations when different channel materials are used, namely brass and silicon. Velocity profiles have been also obtained by a μ -PIV system, while the thickness of the liquid film and the shape of the interface were also determined using the μ -PIV system. It was proved that the shape of the interface can be predicted with reasonable accuracy by the previously proposed correlations. Also the film thickness can be predicted with acceptable accuracy provided that some of the constants are modified according to the material of the test section.

Keywords: Micro Reactor, Falling Film, μ -PIV

1. Introduction

The development of microfluidics is the outcome of the efforts done during the last decades under the concept of process intensification. This new technology offers great advantages like enhanced heat and mass transfer capabilities and the ability to handle very small volumes of fluid. Despite the growing scientific interest and the numerous published works about microfluidics, the mechanisms of fluid flow in microchannels are not completely understood and especially for the case of multiphase flows. The large surface to volume ratio provided by microfluidic devices disrupts the force balance as it is known for flows in macroscale. As a result the well-known correlations of the macroscale are not expected to be valid in the microscale. Thus in order to develop efficient microdevices, design engineers need, new design correlations that would be applicable in the microscale.

This work is focused on the *Falling Film Microreactor (FFMR)*, one of the most important microfluidic devices for gas-liquid ap-

plications. In these devices extended specific surfaces (up to $20,000\text{m}^2/\text{m}^3$) can be obtained while it is important that in *FFMRs* the liquid film remains stable over a wide range of gas and liquid flow rates (Ziegenbalg et al., 2010). Many recently published papers deal with processes that take place in falling film microreactors like absorption of CO_2 by a NaOH aqueous solution (Chasanis et al., 2010; Al-Rawashdeh et al., 2008), micro-distillation and micro-evaporation (Moschou et al., 2013), or separation of binary mixtures of ethanol and n-propanol (Monnier et al., 2012). In all these works there is need for estimating the mass and heat transfer coefficients. To accomplish this, we must be able to predict the geometrical and hydrodynamic characteristics of the liquid phase, namely the film thickness, the shape and the extent of the gas-liquid interface, the velocity profiles and the average velocity. In most cases these parameters are either estimated by correlations valid in the macroscale (i.e. Nusselt correlation for film thickness) or are totally ignored (i.e. the shape of the interface) resulting to inaccurate predictions of mass and heat transfer rates. Only few

works about *FFMRs* hydrodynamics are available in the literature, while they mostly concern liquid film thickness distribution (Yeong et al., 2006; Tourvieille et al., 2013) or the characteristics of the gas-liquid interface (e.g. Yeong et al., 2006) but generally none of the aforementioned works proposes a strategy for designing a *FFMR*.

Driven by the necessity for new design correlations a systematic investigation of the liquid phase hydrodynamic characteristics in *FFMRs* has been conducted in our laboratory in the last years (e.g. Anastasiou et al., 2013a). During this research the effect of various fluid parameters (e.g. physical properties of the liquid phase, flow rate), as well as geometrical characteristics and inclination angle of the conduit on the geometry of the liquid phase and on the velocity profiles have been experimentally investigated. Based on these experimental results two design correlations have been formulated for the prediction of both the shape of the gas-liquid interface the film thickness.

For all the cases studied it was found that the shape of the interface can be described with relative accuracy by a simple second order polynomial (Anastasiou et al., 2013):

$$Y = AX + BX^2 + C \quad (1)$$

where the parameters A , B and C depend only on the geometrical characteristics of the microchannel, namely its width (W_o), and the thickness of the liquid film (H) (**Figure 1**).

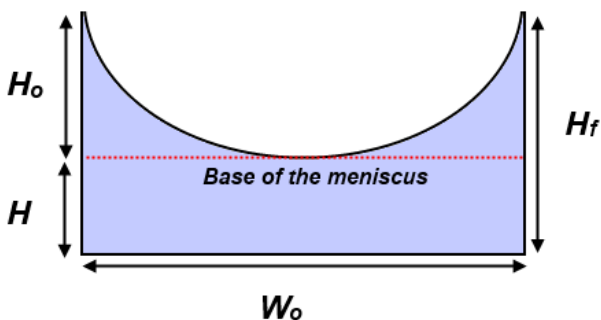


Figure 1: Geometric characteristics of the liquid film (H : film thickness, H_o : meniscus height, H_f : height of the three phase contact line).

An important parameter for the design of *FFMRs* is the thickness of the liquid film (H). The experiments proved that the film thickness

strongly depends on the properties of the liquid phase as well as the width and the inclination angle of the microchannel. Based on the experimental findings, and by performing dimensional analysis it was found that the film thickness is a function of three dimensionless numbers namely: Reynolds (Re), Capillary (Ca) and Froude (Fr). Thus the following correlation for the prediction of film thickness was proposed (Anastasiou et al., 2013a):

$$\frac{H}{W_o} = C(Re^a Ca^b Fr^d)^f \quad (2)$$

The constants a , b , d , f and C can be estimated after fitting on the experimental results while the dimensionless numbers can be estimated by the following equations:

$$Re = \frac{Q\rho}{(\mu h)} \quad (3)$$

$$Ca = \frac{\mu Q}{(W_o h \sigma)} \quad (4)$$

$$Fr = \frac{Q^2}{g_\varphi W_o^3 h^2} \quad (5)$$

The aforementioned correlations (**Eqs. 1 & 2**) are based on data originated from *PMMA* microchannels with various widths using several fluids. The aim of the present work is to investigate the effect of channel material on the geometrical characteristics of the liquid film (i.e. shape of the interface and film thickness) by conducting experiments using different channel materials, namely metal (brass) and silicon. The validity of the previously proposed correlations will be also checked and if necessary they will be modified accordingly.

2. Experimental setup

The experimental setup (**Figure 2**) consists of a fluorescence μ -PIV system, the test section, i.e. the microchannels, and a syringe pump for generating the flow. The first test section consists of three microchannels of square cross-section (1200, 600 and 300 μ m) (**Figure 3**) and is constructed on a sheet of brass using ultra high precision micromachining techniques (Anastasiou et al., 2013b). In

particular a five-axis ultra-precision micro milling machine (Anastasiou et al., 2013b) developed at Brunel University has been used to ensure minimal surface roughness and straightness of the channels. In order to assure continuous free flow, the liquid phase enters by overflowing a circular region preceding the inlet of each microchannel. This test section is similar with the one used in the work of Anastasiou et al. (2013a) which was constructed by PMMA.

Silicon microchannels of rectangular cross-section ($500\mu\text{m } W \times 450\mu\text{m } D$) were fabricated by photolithography and deep reactive ion etching; a photoresist layer (SPR 220-7) was spin coated on a silicon wafer at 4000rpm, followed by a soft bake at 110°C . This was followed by UV exposure, where the microchannel pattern was transferred from a photomask to the photoresist using a contact aligner (Quintel Q4000-6). The pattern was then developed using a standard photoresist developer (Microposit MF-26A) and etched by deep reactive ion etching (STS ASE). The etched depth was measured precisely using a surface profiler (Dektak XT).

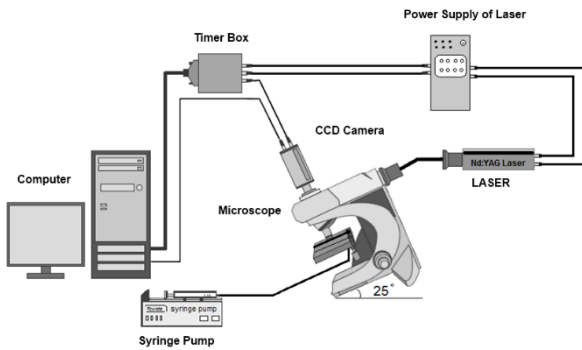


Figure 2: μ -PIV setup.

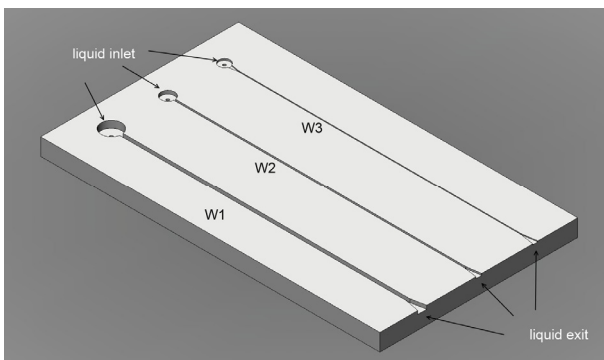


Figure 3: Test sections used for the experiments.

The measuring section of the microchannels was illuminated by a double cavity *Nd:YAG* laser emitting at 532nm. The flow was recorded using a high sensitivity *CCD* camera (Hisense MkII of DantecDynamics), connected to a Nikon (Eclipse LV150) microscope, whose stage can be moved along the vertical axis with accuracy of one micron. The light source is synchronized with the camera shutter by a timer box while the flow was traced by adding Nile red fluorescent carboxylate microspheres (InvitrogenTM) with mean diameter of $1\mu\text{m}$. To obtain sufficiently magnified images a 20X air immersion objective with $NA=0.45$ was used, which results to $3\mu\text{m}$ depth of field. The time delay between frames is in the range of 150-1500 μs , depending on the respective flow rate, while the sampling rate is 5Hz. The interrogation areas for the velocity analysis are 32×64 pixels and the overlapping is 50% for both directions (horizontal and vertical). The image processing and velocity estimation was performed using the Flow Manager Software (Dantec Dynamics[®]).

An aqueous solution of glycerol 30% v/v (*g1*) was used for investigating the effect of viscosity while an aqueous solution of butanol 5% v/v (*b1*) has been used for examining the effect of surface tension. Also distilled water (*w*) has been used as reference fluid. The properties of the liquids used, i.e. the density (ρ), the surface tension (σ) measured by a tensionmeter (Cam200 optical contact angle meter), and the viscosity (μ), measured with an Oswald (Schott Gerate) viscometer, are given in **Table 1**. These properties were measured at room temperature ($23\text{-}25^\circ\text{C}$) while the experiments were conducted under the same conditions. The fluid was circulated by a syringe pump (ALLADIN 2000), while the test section was placed at an inclination angle of 25 degrees from the horizontal position. To eliminate entrance phenomena all the measurements

Table 1: Physical properties of the fluids used.

index	Liquid	μ (cP)	ρ (kg/l)	σ (mN/m ²)
<i>w</i>	<i>Water</i>	1.00	0.99	72.0
<i>g1</i>	<i>Glycerol 30%w/w</i>	1.80	1.03	70.8
<i>b1</i>	<i>Butanol 5%v/v</i>	0.98	0.99	45.0

were performed 40mm downstream from the inlet of the microchannels for the metal test section and 20mm for the silicon one.

The μ -PIV technique, a method intended for velocity measurements in micro-conduits, was also used for assessing the geometrical characteristics of liquid films in microchannels. In this technique the presence of the tracing particles helps in identifying the existence of the liquid phase. Detailed information on the measuring method is given by Anastasiou et al. (2003b). By applying the above technique we were able to measure both the thickness of the liquid film and the velocity of the liquid phase, as well as to reconstruct the shape of the gas-liquid interface. For our measuring system (i.e. type of microscope and objective lenses) it was found that the accuracy of this technique is better than $\pm 2.5\mu\text{m}$ provided that the refractive index of the working fluids is taken into account. A main advantage of this is technique it the utilization of the same experimental setup both for measuring the velocity and for investigating the geometrical characteristics of the liquid film.

3. Results

As it was expected the gas-liquid interface has the shape of a meniscus and this is attributed to the hydrophilic nature of the materials and to the greater relative effect of the capillary forces in such small conduits. For the case of the metal test section and the wider microchannel ($1200\mu\text{m}$) it was observed that the three phase contact line (TPC) is pinned at the same height for the entire flow range studied, which is the result of the contact angle hysteresis phenomenon. A quite different behavior is observed for the $600\mu\text{m}$ width microchannel. For low flow rates the meniscus height (H_o) is almost equal to the film thickness (H). By increasing the flow rate the height of the meniscus is reduced and the interface tends to become a flat surface. A further increase of the flow rate causes a deformation of the interface and now the TPC is pinned at a higher point. A new meniscus is now formed whose curvature is greater than the ones before surface deformation. This behavior is similar to what was found in a previ-

ous work for the *PMMA* test section (Anastasiou et al., 2013a). **Figure 4** presents the shape of the meniscus for the metal the *PMMA* and the silicon test sections. Although the general shape of the meniscus is the same, the *TPC* in the metal test section is located at lower position, for the same flow rate. This can be attributed to the greater contact angle at the metal test section, i.e. 62° for *PMMA* and water compared to 78° for the metal and water.

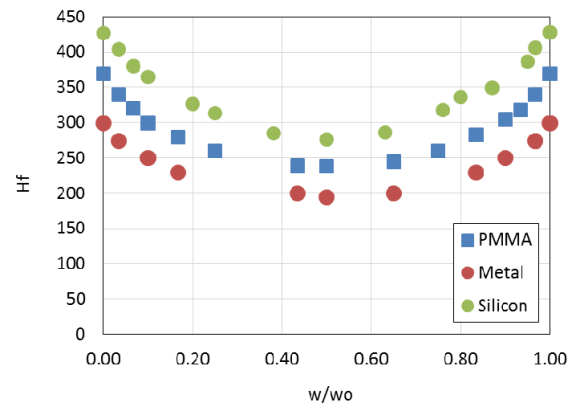


Figure 4: Effect of microchannel material on the meniscus shape (water and $Q_n=33 \text{ ml}/(\text{h}\cdot\text{mm})$).

The same experiments have been conducted for the silicon test section. It was found that in this case the *TPC* is pinned at the top edge of the microchannel even for low flow rates. This is reasonable considering the swallow depth of the particular microchannel. For low liquid flow rates the curvature of the meniscus is high. As the flow rate increases the curvature decreases and the interface tends to be flat. A further increase of the flow rate results reversed curvature of the interface (**Figure 5**).

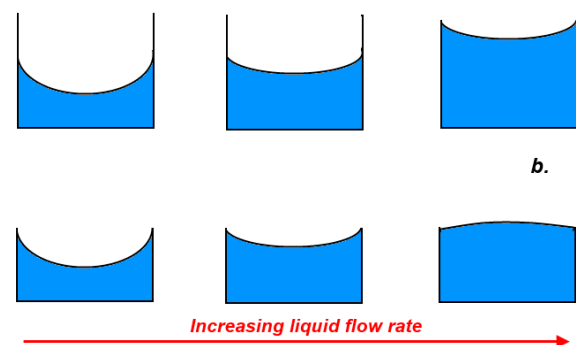


Figure 5: Shape of the interface a) metal microchannel ($W_o=600 \mu\text{m}$) b) silicon microchannel ($W_o=500 \mu\text{m}$).

In **Figure 6** reconstruction data from both test sections, in dimensionless form, are compared with the correlation for the prediction of the meniscus shape (**Eq. 1**). The proposed correlation is in good agreement with the experimental data which means that in general the meniscus shape is not considerably affected by the type of material. Thus **Eq. 1** can be regarded a useful tool for the estimation of the interfacial area in *FFMRs*.

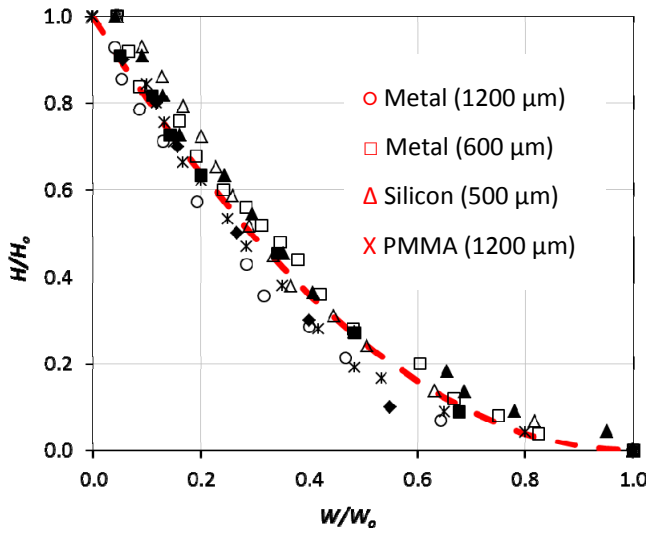


Figure 6: Comparison of Eq. 1 with the experimental data for the meniscus shape.

It is clear that for the case of the metal test section thinner films (about 16%) were measured while the same behavior was observed for all the fluids tested. Also as it was expected for the *gl* fluid, which is the most viscous, the thickest films were measured while the solution *b1* formed films almost of the same thickness with the water.

Using the same experimental setup the thickness of the liquid film was also measured. In **Figure 7** a comparison between the data for the metallic test section and older findings for the *PMMA* (Anastasiou et al., 2013a) is made. For the comparison film thickness is presented as a function of the normalized flow rate Q_n :

$$Q_n = \frac{\text{volumetric flow rate}}{\text{microchannel width}}$$

In **Figure 8** the results for the various tests sections are presented. It is depicted that in the silicon test section thicker films are formed

compared with what it was measured in the 600 μm *PMMA* microchannel and the metal test section. This behavior can be attributed to many factors. First of all the width of the silicon microchannel is 500 μm which means that is narrower than the *PMMA* one and as it was proved in a previous work (Anastasiou et al., 2013a) film thickness increases dramatically with the reduction of the width. Moreover the silicon microchannel is shorter than the other two test sections and thus the measurements could be affected by inlet and outlet phenomena.

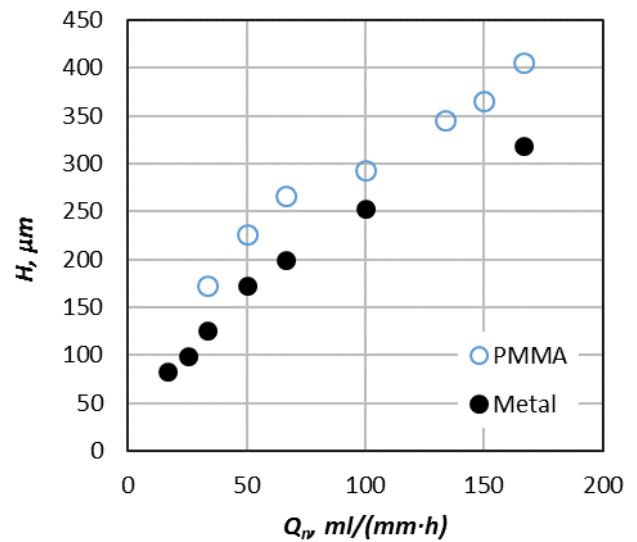


Figure 7: Effect of micro-channel material on the film thickness (water in the 1200 μm microchannel).

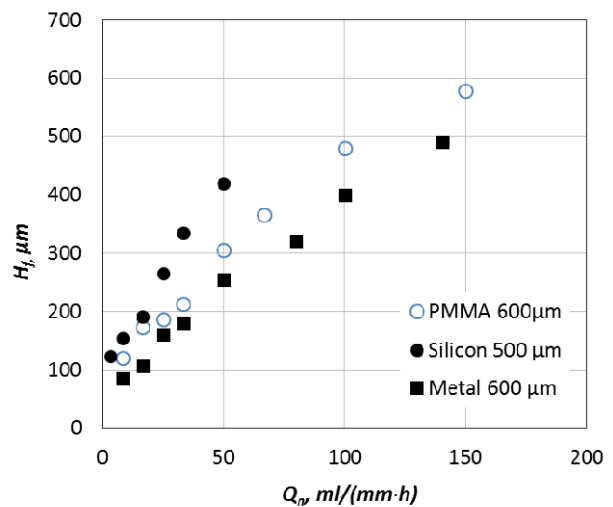


Figure 8: Effect of micro-channel material on the meniscus height for water.

The experimental data for film thickness were compared with the predictions of *Eq. 2*, whose constants were suitably adjusted. For the case of the metal test section the difference between the experimental results and the predictions of *Eq.2* was higher than 45%. Nevertheless, by adjusting constant *C* from 3.04 to 2.4 (and by keeping *a*, *b*, *d* & *f* stable) it seems that the deviation between the experimental and the predicted values is less than 15% (*Figure 9*).

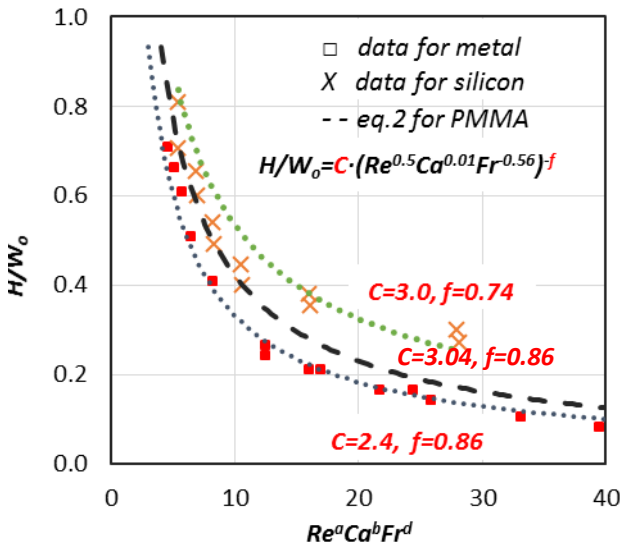


Figure 9: Prediction of film thickness using *Eq.2*. Comparison with experimental data.

On the other hand for the silicon test section it was found that in order to have satisfactory predictions from *Eq. 2* both the constants *C* and *f* should be adjusted. Thus by setting *C* to 3.0 and *f* to 0.74 acceptable accuracy can be achieved (uncertainty better than 15%). In *Table 2* the values of the coefficients *a*, *b*, *d*, *f* and *C* are summarized for all the cases studied.

Table 2: Coefficients of *Eq. 2* for all cases studied.

material	<i>a</i>	<i>b</i>	<i>d</i>	<i>F</i>	<i>C</i>
PMMA				0.86	3.04
Metal	0.50	0.01	-0.56	0.86	2.40
Silicon				0.74	3.00

As the flow rate increases the “*M*”-profile decays and eventually it turns to be parabolic for high liquid flow rates. This “*M*”-profile has been already recognized in a previous work

(Anastasiou et al., 2013a) and its presence has been related to the geometrical characteristics of the liquid film. Specifically this velocity profile is observed when the H_0/H ratio (*Figure 10*) is higher than 1. It has been confirmed that this criterion is also valid for the metal test section.

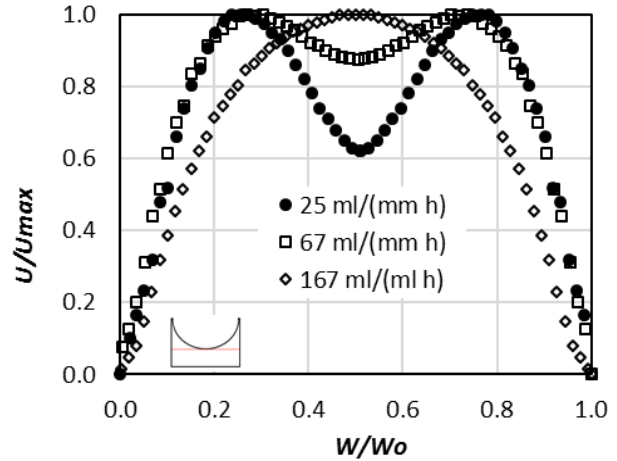


Figure 10: Velocity profiles for the 1200 μm width microchannel (water, metal test section).

However, when the silicon microchannel was tested the velocity profiles were always parabolic (*Figure 11*) regardless of the liquid flow rate. The absence of the “*M*”-profile in that case is probably related to the high H_0/H ratio as for this channel the thickest liquid films measured.

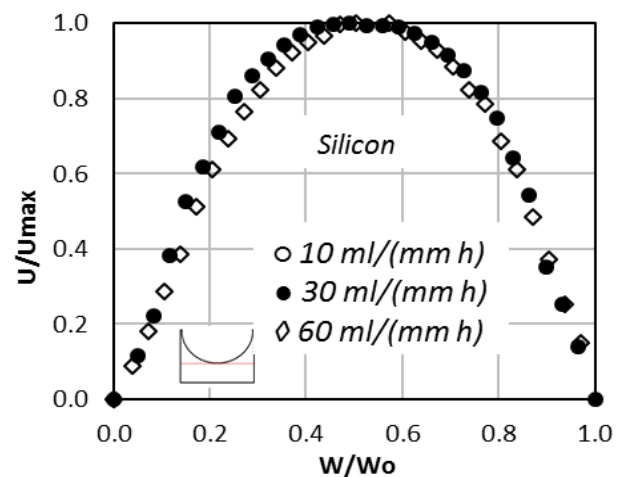


Figure 11: Velocity profiles for the silicon microchannel (500 μm) for various flow rates (water).

4. Conclusions

This work is part of a broader investigation of the geometrical and hydrodynamic characteristics of the liquid film in falling micro reactors. Our aim was to check the validity of previously formed correlations for the prediction of the film thickness and the shape of the gas-liquid interface. To accomplish this, experiments have been conducted in two test sections constructed by different materials, namely brass and silicon. The most important results can be summarized to the following:

- The shape of the flowing meniscus can be described by the empirical correlation (**Eq. 1**) with acceptable accuracy for all the test sections studied.
- It is also confirmed that the appearance of the “*M*”-profile is related to geometrical characteristics of the liquid film and specifically to the ratio H_o/H .
- It was proved that the proposed correlation (**Eq. 2**) can predict the film thickness with reasonable accuracy (uncertainty less than 15%) by suitably adjusting the equation constants. More specifically, it was found that two of the constants in **Eq. 2**, namely C and f , depend on the material of the microchannel. More work is certainly needed in order to investigate the dependence of constants C and f on the aforementioned characteristics and also from parameters as the cross section of the microchannels and the aspect of its dimensions.

Further experiments must be performed using micro-channels made of other type of materials and whose cross sections have different characteristics, e.g. circular, trapezoidal, rectangular etc.

Acknowledgements: The authors wish to acknowledge Prof. S.V. Paras (*AUTH*) and Dr. H. Makatsoris (*Brunel Univ. UK*) as well as our Lab technician Mr. A. Lekkas (*AUTH*) for their contribution.

Notation

g	acceleration of gravity, m/s^2
h	depth of the microchannel, μm
H	liquid film thickness, μm
H_f	height of the three phase contact line, μm
H_o	meniscus height, μm
h	depth of the microchannel, μm
Q	liquid flow rate, ml/h
Q_n	normalized liquid flow rate, $ml/(mm \cdot h)$
TPC	three phase contact line, -
U	liquid velocity, m/s
U_s	superficial liquid velocity, m/s
W_o	width of the microchannel, μm

Greek Symbols

μ	liquid viscosity, $mPa \cdot s$
σ	surface tension, N/m
ρ	liquid density, kg/m^3

5. References

- Al-Rawashdeh, M.M., Hessel, V., Lob, P., Mevissen, K. & Schonfeld, F. 2008. Pseudo 3-D simulation of a falling film microreactor based on realistic channel and film profiles. *Chem Eng Sci*, **63**, 5149-5159.
- Anastasiou, A.D., Gavriilidis, A. & Mouza, A.A. 2013. Study of the hydrodynamic characteristics of a free flowing liquid film in open inclined microchannels. *Chem Eng Sci*, **101**, 744-754.
- Chasanis, P., Lautenschleger, A. & Kenig, E. Y. 2010. Numerical investigation of carbon dioxide absorption in a falling-film microcontactor. *Chem Eng Sci*, **65**, 1125-1133.
- Monnier, H., Portha, J.-F., Kane, A. & Falk, L. 2012. Intensification of heat transfer during evaporation of a falling liquid film in vertical microchannels Experimental investigations. *Chem Eng Sci*, **75**, 152-166.

- Moschou, P., De Croon, M.H., Van Der Schaaf, J. & Schouten, J.C. 2013. Liquid flow rate effects during partial evaporation in a falling film micro contactor. *Chem Eng Process*, **69**, 95-103.
- Tourvieille, J.-N., Bornette, F., Philippe, R., Vandenberghe, Q. & Bellefon, C.D. 2013. Mass transfer characterisation of a microstructured falling film at pilot scale. *Chem Eng J*, **227**, 182-190.
- Yeong, K.K., Gavriilidis, A., Zapf, R., Kost, H.J., Hessel, V. & Boyde, A. 2006. Characterisation of liquid film in a microstructured falling film reactor using laser scanning confocal microscopy. *Exper Therm Fluid Sci*, **30**, 463–472.
- Ziegenbalg, D., Löb, P., Al-Rawashdeh, M.M., Kralisch, D., Hessel, V. & Schönfeld, F. 2010. Use of 'smart interfaces' to improve the liquid-sided mass transport in a falling film microreactor. *Chem Eng Sci*, **65**, 3557-3566.